SSRG International Journal of Electrical and Electronics Engineering
ISSN: 2348-8379/ https://doi.org/10.14445/23488379/IJEEE-V10I10P113

Volume 10 Issue 10, 126-136, October 2023

Original Article

A Miniaturized Square Cavity SIW Dual-Band BPF with Slotted Koch Snowflake Fractal Based Design

Ali A. Abdulhasan[1], Ali J. Salim[2], Jawad K. Ali[3]

[1,2,3]*Communication Department, University of Technology, Iraq.*

[1]*Corresponding Author : Ali.A.Abdulhasan@uotechnology.edu.iq*

Received: 13 August 2023 Revised: 15 September 2023 Accepted: 13 October 2023 Published: 31 October 2023

Abstract *- This article presents a dual-band fractal-based Bandpass Filter (BPF) for Substrate-Integrated Waveguides (SIWs) for the first time. The suggested filter is built by cutting a slit into the structure's top layer, Koch Snowflake fractal style. The Fractional Bandwidth (FBW) at 7.7 GHz for the first band of the downsized BPF is 9.45 percent, while the FBW at 9.65 GHz for the second passband is 8.8 percent. In addition to reducing the SIW cavity's footprint, the downsized filter has improved S-parameter features, such as a narrower upper rejection band and a narrower lower rejection band. The filter's dimensions are approximately 0.917 × 0.917 λg^2 or 21.6 × 21.6 mm^2. The substrate used is Rogers RO4350B, with a relative dielectric constant of 3.48, a loss tangent of 0.0037, and a thickness of 0.762 mm. The validity of the proposed design has been verified through simulations using CST, HFSS, and Sonnet software. A prototype of the BPF has been fabricated and tested, showing good agreement between the predicted and measured results. The work also examines the impact of stub loading and its absence on the isolation between bands and the generation of TZs at 4.26, 8.3, 8.63, 11.66, and 14.2 GHz to enhance the selectivity of the proposed filter.*

Keywords *- Dual-band BPF, Koch snowflake fractal, Substrate Integrated Waveguide (SIW), CST, Sonnet.*

1. Introduction

When connecting waveguides to conventional planar circuits, the state-of-the-art solution is Substrate-Integrated Waveguide (SIW) [1]. In the SIW configuration, the metallic plates are separated by a dielectric layer, and the conductors are connected along the side walls by metallic cylinders [2]. Filters and other microwave components have recently been designed with SIW characteristics in mind [3-5]. These filters are smaller in size and have less loss than their waveguide counterparts, but they are just as effective [6].

In contrast to microstrip designs, however, their parameters are more stringent. To solve this problem, numerous topologies, including the ridge SIW, half-mode SIW, and folded SIW, have been suggested to minimize further the size of SIW structures [7-9]. It's crucial to think about the possibility of shrinking down SIW-using systems. The SIW architecture may be simplified in several ways, some of which are addressed in [10].

As the requirements for compact design in mobile devices become more stringent, the size of SIW Bandpass Filters (BPFs) must be reduced. The design and production of high-quality microwave components have piqued an interest in fractal geometries due to their space-filling and self-similarity features. Actual fractal curves are mathematically impossible, although low-order pre-fractals may do the trick [11]. Several attractive and applicable fractal geometries may be used to address these issues. Miniature SIW bandpass filters based on various fractal geometries have been suggested and built by a few researchers in recent years [12-26].

The ability of highly selective bandpass filters to effectively remove noise from complex multimode mobile systems is increasing their demand. Transmission Zeros (TZs) at absolute frequencies often enhance the filtering skirt. SIW filters may leverage creative coupling topologies [28] and source-load coupling [27] to obtain transmission zeros near the pass band.

A mixed-coupling architecture makes microwave filters with frequency-selectable and limited transmission-zero regions possible on an SIW substrate [29]. Increased selectivity may be achieved by cross couplings in vertically stacked SIW filters [30]. One standard method of growing selectivity is to cascade the filter's unit structure, increasing its order [31]. When fabricating SIW bandpass filters, using resonators with dual-mode operation and dual-band operation might potentially assist in reducing the overall size of the filter [32]. Satellite communications systems have extensively used dual-band filters, including fixed satellite

service, military FSS, terrestrial earth exploration, and meteorological satellite. These filters are essential in RF/microwave systems because they remove interference.

This article simulates and fabricates a miniaturized square cavity SIW dual-band BPF with a slotted Koch snowflake fractal-based design. The proposed filter is designed using Computer Simulation Technology (CST). The validity of the proposed method has been verified through simulations using CST, HFSS, and Sonnet software.

A prototype of the BPF has been fabricated and tested, showing good agreement between the predicted and measured results. The substrate used is Rogers RO4350B, with a relative dielectric constant of 3.48, a loss tangent of 0.0037, and a thickness of 0.762 mm.

In summary, SIW technology allows for integrating waveguides with flat circuits. Filters based on SIWs may be more selective and compact via techniques such as dual-mode/dual-band resonators and fractal geometries.

2. Architecture of the Proposed Fractal

A snowflake fractal begins with a triangle, from which more triangles develop indefinitely. The zeroth, first, second, and third iterations of the von Koch snowflake fractal are seen in Figure 1. After each cycle, more triangles are added to the design. In a closed system, the circumference may hypothetically grow to infinity. It seems to be a contradiction. However, this feature has led us to discover possible uses in microwave circuitry.

The von Koch snowflake is used in the proposed design to examine the electromagnetic properties of a substrate integrated waveguide bandpass filter. A microwave planar filter with high performance was successfully created. The fact that the simulation and measurement of the filter accord so well lends credence to the proposed theory.

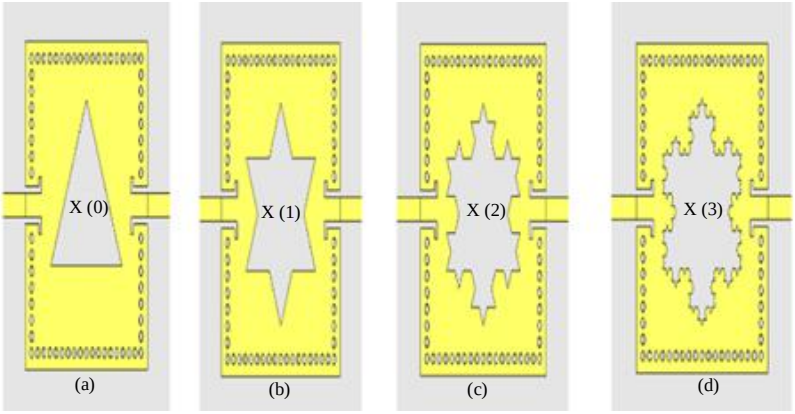

Fig. 1 A diagram depicting the development of an island in a von Koch snowflake fractals (a) Zero-th iteration, (b) First iteration, (c) Second iteration, and (d) Third iteration.

Table 1. The triangles and their corresponding areas incrementally increased with each repetition

Iteration	Area of One Single Triangle	Number of the Added Triangle	Total Area Added
Zero-th	X(0)	1	X(0)
First	(1/9)X(0)	3×4^0	$(3 \times 4^0 \times 1/9)X(0)$
Second	$(1/9^2)X(0)$	3×4^1	$(3 \times 4^1 \times 1/9^2)X(0)$
Third	$(1/9^3)X(0)$	3×4^2	$(3 \times 4^2 \times 1/9^3)X(0)$
N-th	$(1/9^n)X(0)$	$3 \times 4^{n-1}$	$(3 \times 4^{n-1} \times 1/9^n)X(0)$

2.1. Design Procedure

This section presents the development of a dual-band BPF for the Ku and K bands that uses an SIW and operates at 7.7 and 9.65 GHz. As a small filter, the necessary measurements are not more than 21.6 mm by 21.6 mm. The design process may be described as follows: To begin, the size of the desired filter must be determined. An SIW transition form is placed in the filter's middle and is supplied by a pair of microstrip lines. The resonant frequency first establishes the SIW cavity size.

Equations 1 and 2 may be used to determine the resonant frequency (TE_{moq}) of the SIW dual-band filter can be expressed as [33]. For the dual-band SIW to function at the required frequencies, its main dimensions are $W_{eff} = l_{eff} =$ 21.6 mm.

$$f_{101} = \frac{c}{2\pi\sqrt{\mu_r \varepsilon_r}} \sqrt{\left(\frac{\pi}{W_{eff}}\right)^2 + \left(\frac{\pi}{l_{eff}}\right)^2} \quad (1)$$

$$\left\{ \begin{array}{l} W_{eff} = W - \frac{d^2}{0.95p} \\ l_{eff} = l - \frac{d^2}{0.95p} \end{array} \right\} \quad (2)$$

The filter has a dielectric constant Rogers RO4350B of 3.48, a dielectric loss tangent of 0.0037, a conductivity of copper of σ = 5.8 107 S/m, and a thickness of 0.762mm. It was created with the CST software program.

Figure 2 illustrates the basic model of a dual-band SIW BPF configuration. It consists of an SIW square cavity fed by microstrip lines to the SIW transition form at the centre of the cavity. The results indicate that the BPF has four sub-bands with centre frequencies of 5.25, 8.23, 11.74, and 13.64 GHz, each with a different mode in the sub-band, as shown in Figure 3. The filter structure in this design aims to manipulate the first four resonant modes in a SIW cavity and engineer them into two passbands by loading the snowflake Koch slot on the top layer of the proposed filter. The first step in this design involved etching an etched triangle slot as the initiator slot of the proposed fractal, as depicted in Figure 1(a).

Table 2. The parameters for the proposed SIW filter

Parameter	l_{eff}	W_{eff}	d	p	l_{slot}	w_{slot}	l_f
Value (mm)	21.6	21.6	0.7	1.2	2.7	0.5	1.2

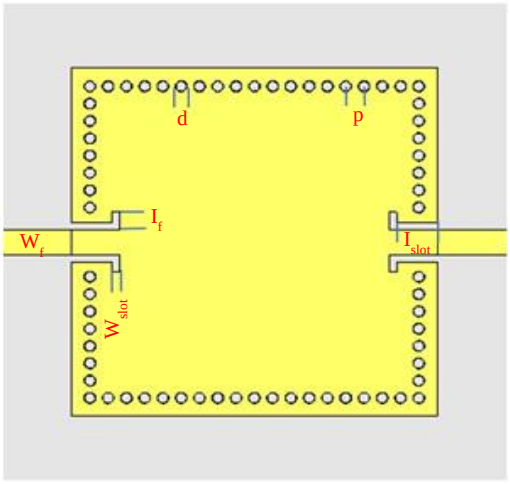

Fig. 2 The fundamental structure of dual-band SIW BPF

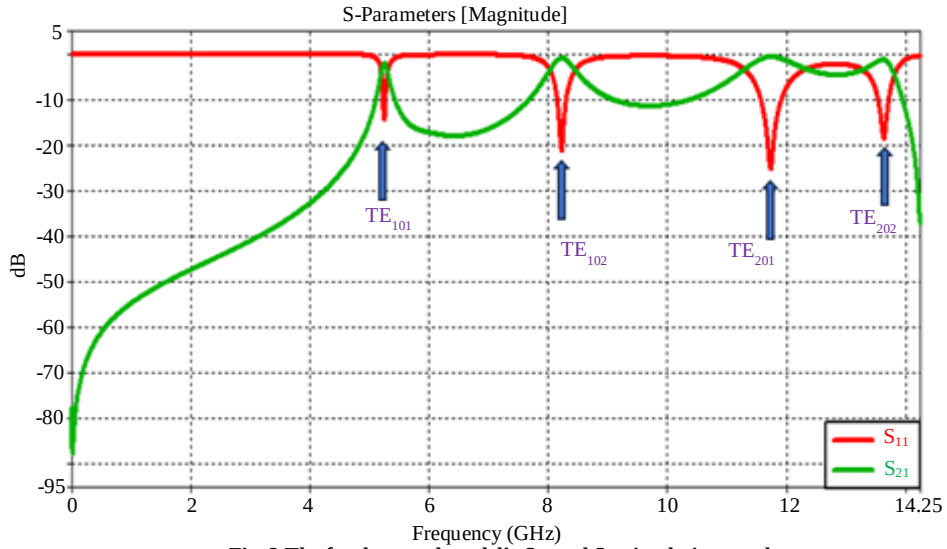

Fig. 3 The fundamental model's S_{11} and S_{21} simulation results

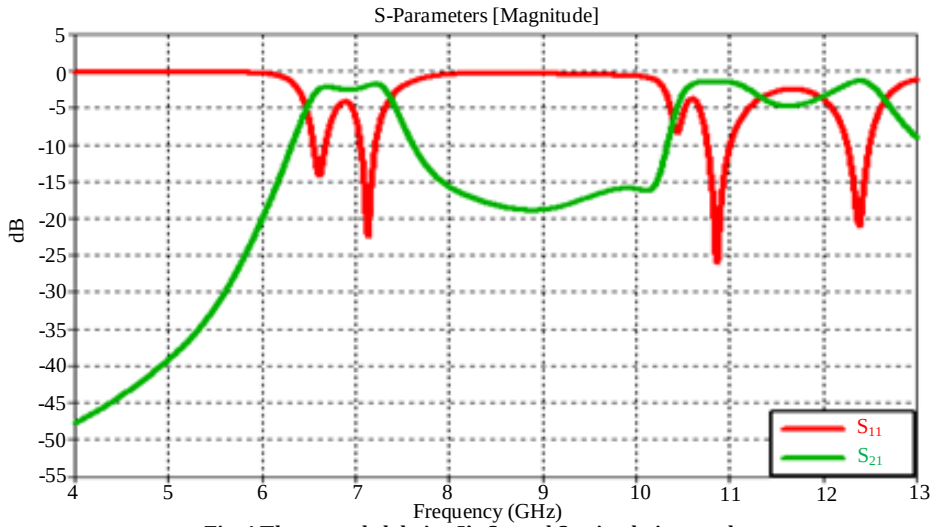

Fig. 4 The upgraded design I's S_{11} and S_{21} simulation results

Remarkably, the TE_{101} mode and TE_{201} mode undergo mode shifting during the slot-developing process of von Koch snowflake fractals, bringing them near the TE_{102} mode and TE_{202} mode, respectively, thus generating two passbands. According to Figure 4, the first passband is produced due to the near convergence of modes TE_{101} and TE_{102}.

The second stage is to apply the required fractal geometry's first iteration, as illustrated in Figure 1(b), and the suggested filter's second band is formed due to the approaches of modes TE_{201} and TE_{202}. As a result, Figure 5 depicts the centre frequencies of the dual bands (7.7 and 10.26 GHz, respectively).

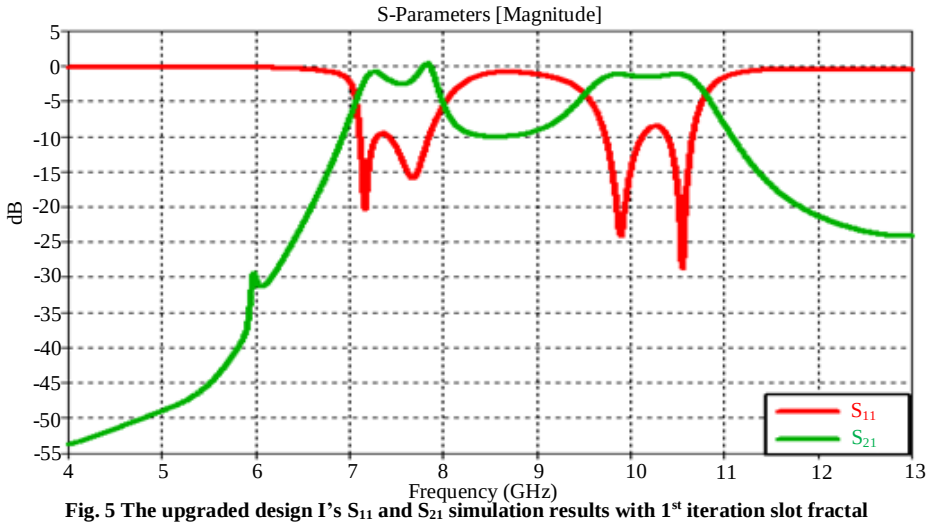

Fig. 5 The upgraded design I's S_{11} and S_{21} simulation results with 1st iteration slot fractal

The next step involves applying the snowflake Koch's slot in its second iteration, as shown in Figure 1(c).

Each iteration of the fractal increases the length of the slot on the top layer, which extends the equivalent electric length of the Substrate-Integrated Waveguide filter. Figure 6 demonstrates the frequency shift in the second passband of the Substrate-Integrated Waveguide (SIW) filter. The frequency has changed from 10.26 GHz to 9.9 GHz, while the first passband remains unaffected. The final step in enhancing design I was to load the third iteration slot fractal, as illustrated in Figure 1(d). The results shown in Figure 7 indicate that the first band remains unchanged while the second band shifts from 9.9 GHz to 9.65 GHz.

The resonant frequency is almost fixed for the first pass range and does not depend on the number of iterations of the fractal slot. However, the resonant frequencies of the second band move to the lower side of its centre frequency.

Furthermore, the miniaturized filter exhibits enhanced S-parameter characteristics, such as a high lower and upper rejection band, resulting in increased compactness of the SIW cavity.

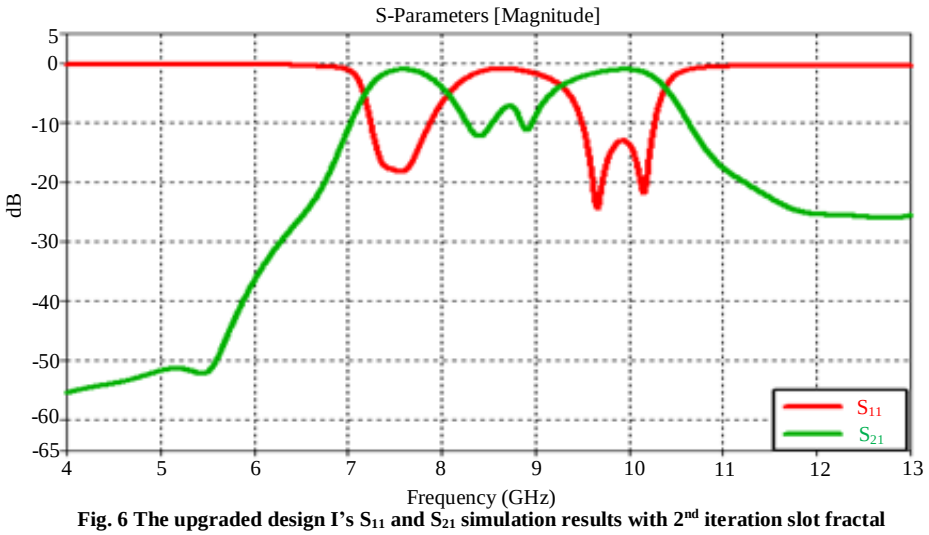

Fig. 6 The upgraded design I's S_{11} and S_{21} simulation results with 2nd iteration slot fractal

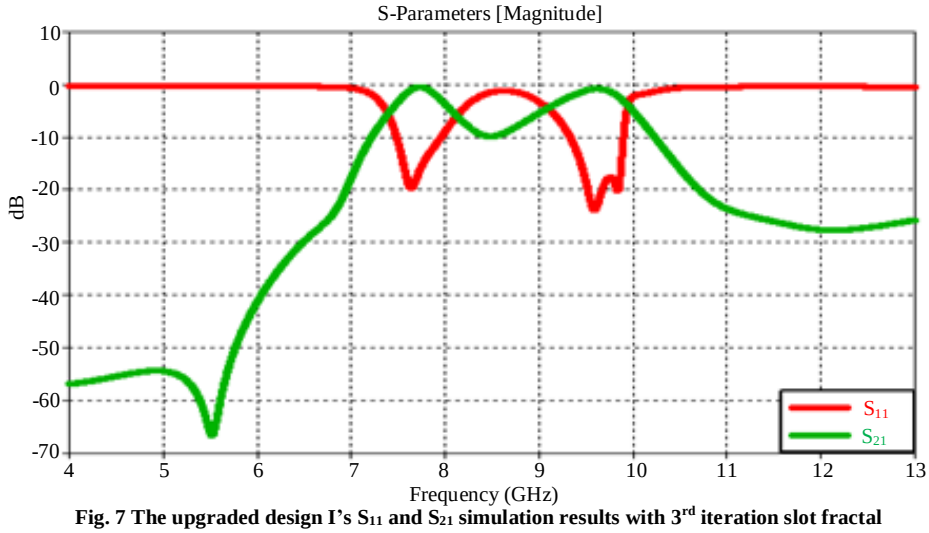

Fig. 7 The upgraded design I's S_{11} and S_{21} simulation results with 3rd iteration slot fractal

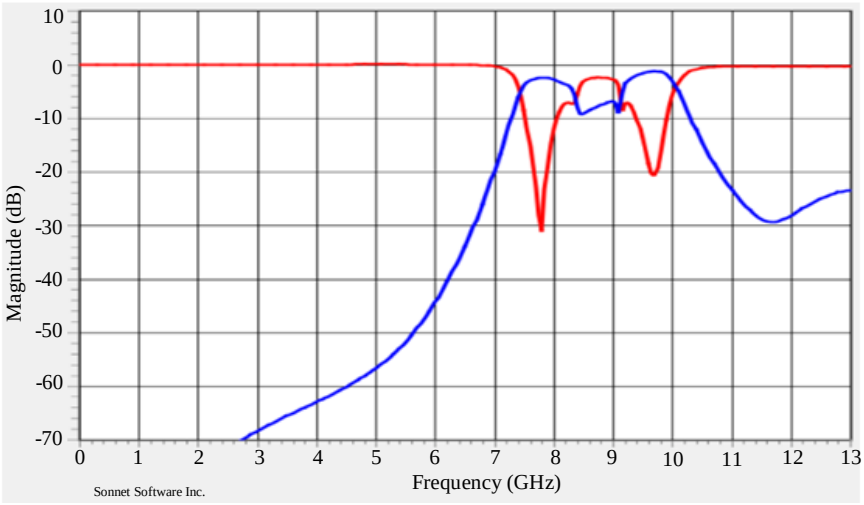

Fig. 8 The return loss and transmission responses of the proposed filter using Sonnet V. 17.56

CST microwave studio was used to simulate the filter construction seen in Figure 1(d). Figure 7 shows the results of the simulations for the insertion and return losses.

CST microwave studio uses the Moments (MoM) technique for electromagnetic analysis. The findings from CST microwave studio were verified by applying the same design concepts to the filter setup shown in Figure 1(d) in the Sonnet V.17.56 simulator. Figure 8 displays the results of the simulations for the insertion and return losses. The Finite Element Method (FEM) numerical approach is also used by Ansys electronics desktop 2022 R1 to verify the response further. Figure 9 shows the results of the simulations for the insertion and return losses.

Fig. 9 The return loss and transmission responses of the proposed filter using Ansys electronics desktop 2022 R1

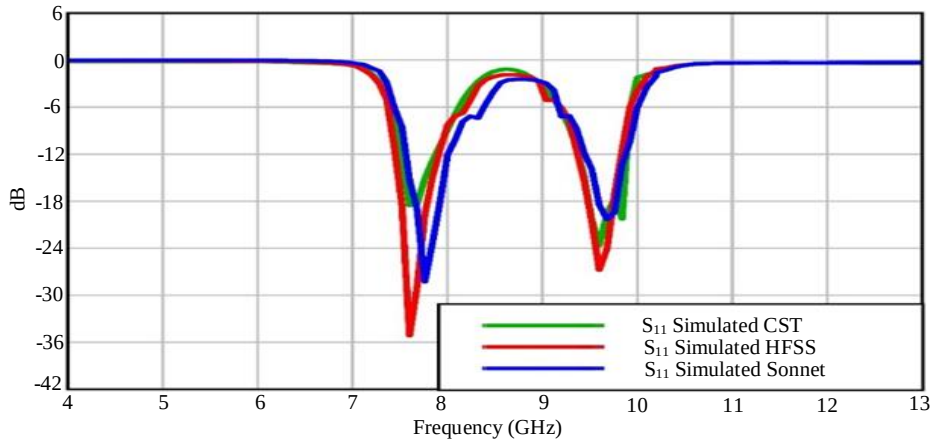

Fig. 10 Return loss responses of CST, HFSS and Sonnet simulators for the proposed filter

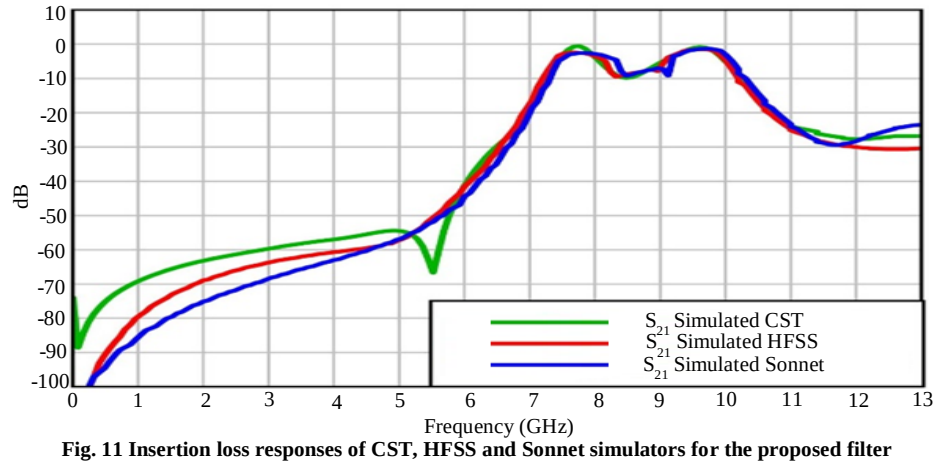

Fig. 11 Insertion loss responses of CST, HFSS and Sonnet simulators for the proposed filter

Figures 10 and 11 show the magnitudes of S-parameter simulation results produced from CST, Sonnet, and HFSS, which may be used to evaluate the simulation results' correctness. These graphs compare simulation results from several commercial software packages processed via the proposed filter, highlighting the most similar simulation results.

3. Fabrication of the Filter and Experimental Results

Based on the analysis and simulation conducted using CST microwave studio, A prototype of a dual-band Substrate Integrated Waveguide (SIW) Bandpass Filter (BPF) based on the slotted snowflake Koch fractal has been successfully built.

The fabrication was done using a Computer numerically Controlled machine (CNC) in the microwave laboratory. The photograph of the fabricated prototype is depicted in Figure 12. Subsequent measurements were performed using a Vector Network Analyzer (VNA), as shown in Figure 13.

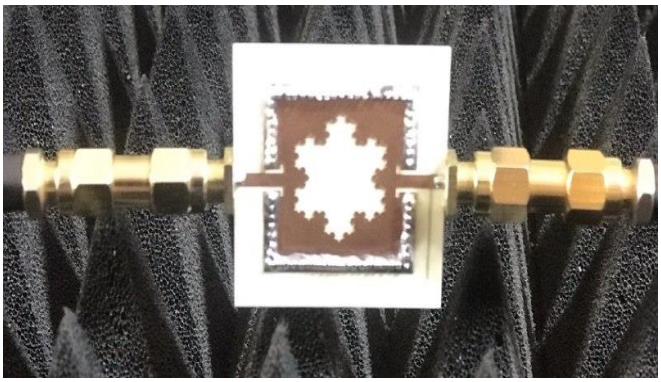

Fig. 12 A photograph of the manufactured SIW bandpass filter is depicted in figure (1-d)

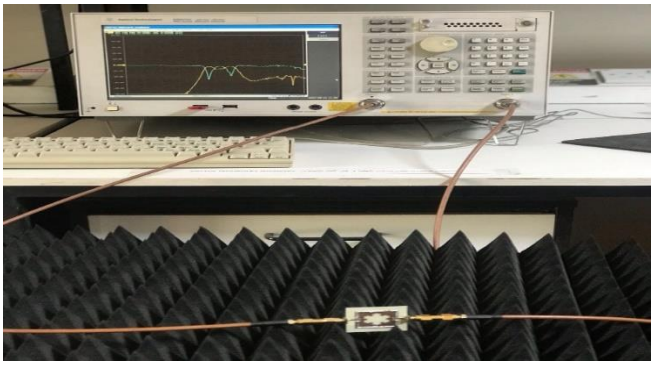

Fig. 13 Fabricated dual band SIW BPF measurement

Figures 14 and 15 display the simulated and measured values of the input reflection coefficient (S_{11}) and transmission coefficient (S_{21}), respectively. The results indicate significant agreement between the simulated and measured outcomes. However, slight variations between the measured and simulated results may be attributed to tolerances inherent in the substrate's properties. The in-band responses demonstrate that changes in ε_r lead to frequency shifts, while changes in tanδ cause attenuation shifts. Moreover, manufacturing tolerances in the filter's construction contribute to the inaccurate placement of resonant bands.

Additionally, insufficiencies in the SMA or transition can impact the evaluation. The observed ripple was primarily caused by calibration issues with the measuring devices. These discrepancies can be principally attributed to conductor loss, connector mismatches, and fabrication tolerance, as discussed in Section 4.2.5. Consequently, this may result in increased attenuation. The final filter size measures 0.917 × 0.917 λ_g^2 or 21.6 × 21.6 mm^2. The results from both the fabrication and the simulations are compared in detail in Table 3.

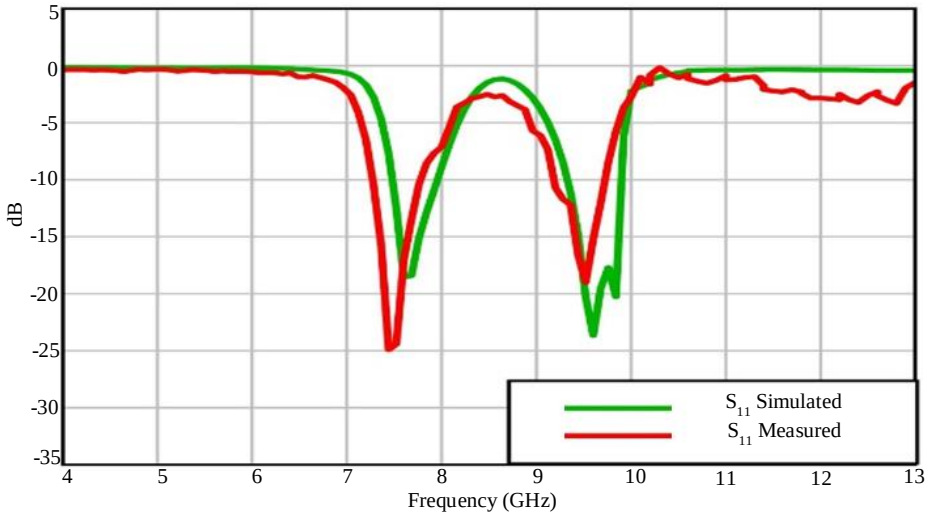

Fig. 14 Return loss responses of the experimental and CST simulator for the proposed filter

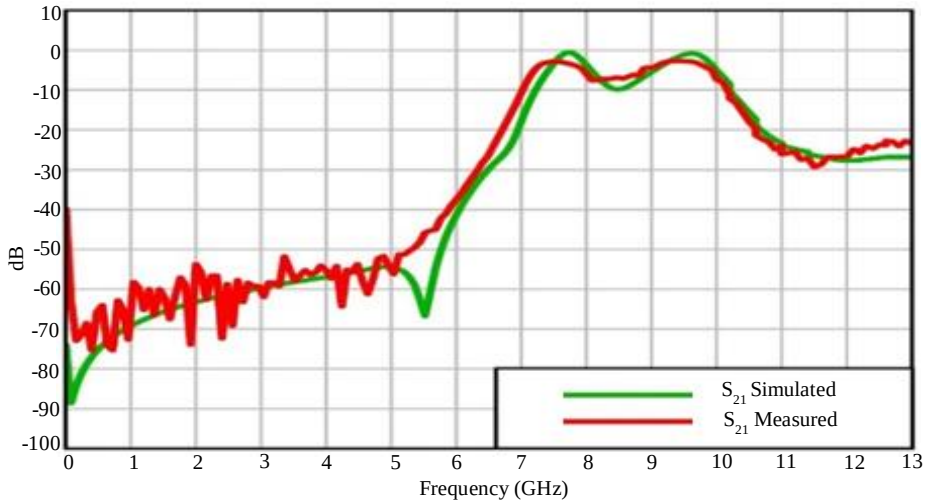

Fig. 15 Insertion loss responses of the experimental and CST simulator for the proposed filter

Table 3. The simulated and measured results summary

Bands		Centre Frequency f_0 (GHz)	S-Parameter		FBW%
			RL(dB)	IL(dB)	
1	Simulated	7.7	19.55	0.88	9.45%
	Measured	7.6	24.5	2.9	11.2%
2	Simulated	9.65	17.86	1.18	8.8%
	Measured	9.52	18.7	2.7	10.25%

3.1. Final Design Refinement

The most crucial feature of passive planar filters is the rejection band to eliminate the harmonics associated with the passband, while the other characteristics represented by losses (IL and RL) are at a minimum acceptable level in communications systems because the amplifiers amplify the power of the received signal after passing it through the filter. The lower and upper rejection bands are good, but the isolation between bands needs to improve, as shown in Figure 16. Add ($L_{stub1} = \lambda_g /4$) stub load as a band stop to improve the isolation band from 10 to 20 dB, and also, add ($L_{stub2} = \lambda_g /2$) stub load as a bandpass as shown in Figure 17, to generate TZs at frequencies of 4.26, 8.3, 8.63, 11.66, and 14.2 GHz with a rejection of 77.4, 24.7, 44.2, 49.1, and 43.4 dB respectively. These modifications aim to increase the selectivity of the proposed filter shown in Figure 17.

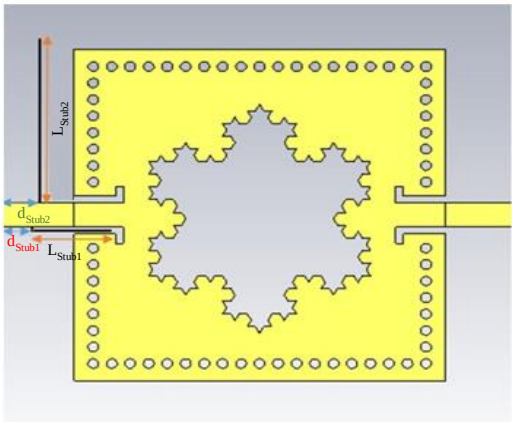

Fig. 16 Design II of the dual-band SIW BPF configuration's enhanced version

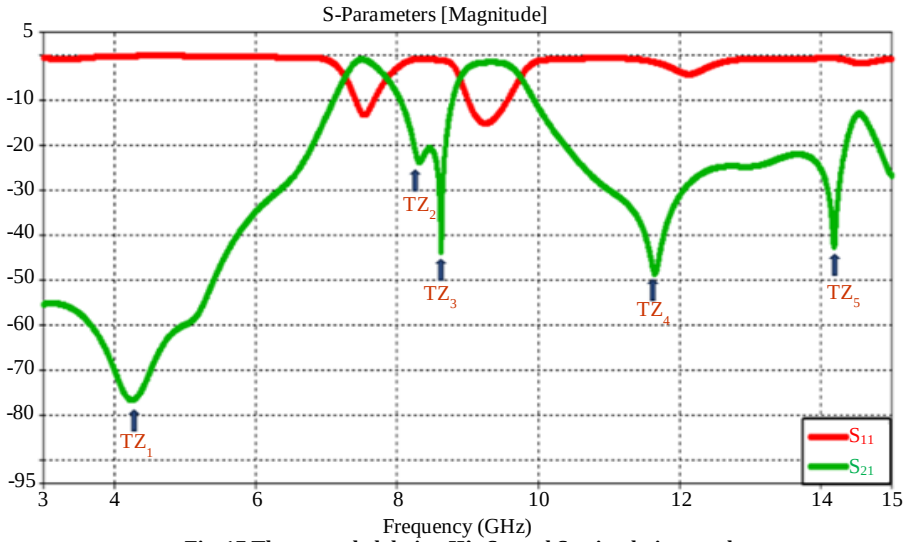

Fig. 17 The upgraded design II's S_{11} and S_{21} simulation results

Table 4. Stubs load parameters

Parameter	L_{stub1}	L_{stub2}	d_{stub1}	d_{stub2}	w_{stub}
Value (mm)	5.47	11.95	1.85	2.35	0.1

3.2. Surface Current Distributions

The electric current density distribution on the surface of the modelled filter at five distinct frequencies, namely the design frequencies, 7.7 and 9.65 GHz, while three other frequencies are illustrated in Figure 18. The filter's surface exhibits no currents at 4.25,8.5 and 11.64 GHz, considered out-of-band. The current density observed on the filter's surface at 7.7 and 9.65 GHz suggest that the passbands will experience a current flow with density.

On the other hand, the level of symmetry exhibited by the current densities is being considered. The entirety of the filter surface serves as a representation of the filter response measurement in Figure 18.

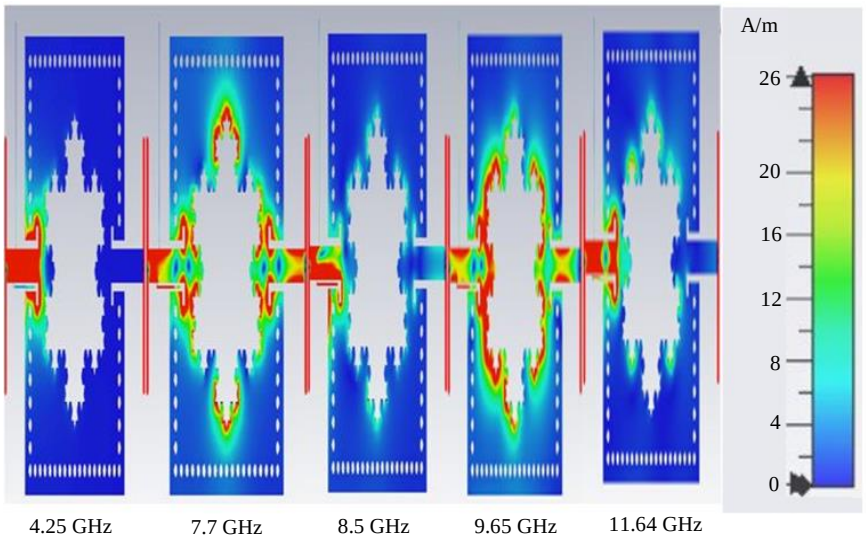

Fig. 18 The surface current distribution on the snowflake Koch fractal-based SIW BPF at 7.7 and 9.65 GHz, also three other frequencies below and beyond the design frequencies

Table 5. Comparative analysis of the performance of the suggested filter concerning previous relevant studies

Reference	f_0 (GHz)	IL/RL (dB)	A Fractal-Based Method	Size (mm×mm)
[13]	6.5	2/12	SIW	8.5×17
[14]	1.12	0.71/13	HMSIW	27.8×28.8
[15]	4.67	1.2/24	QMSIW	17.4×17.4
[16]	3.4	1.8/11.4	HMSIW	66×10
[17]	9.2	1.05/22	SIW+DGS	16×16
[18]	3.65	1.02/25	QQMSIW	20×53
[19]	6.15	1.4/21	QEMSIW	11×17
[20]	2.4	1.45/21	SIW+OCSRR	10.4×5.2
[21]	11.185	0.82/24.8	FSIW	11.5×5.4
[22]	5.5	0.75/23	SIW+MM	7.5×8
[23]	3.5	1.1/16	HMSIW+DGS	42.5×4.5
[24]	6.4	2.5/32	SIW+DGS	21.5×13.38
[25]	5.2	1.1/14.5	HMSIW+DGS+CSRR	27.8×7.25
[26]	3.25	2/20	HMSIW+DGS	50×12
Proposed Filter	7.7/9.65	0.88/19.55, 1.18/17.86	SIW	21.6 × 21.6

4. Conclusion

The third iteration of the Koch snowflake fractal is studied to suggest and develop a miniaturized Substrate-Integrated Waveguide (SIW) Bandpass Filter (BPF).

The proposed filter in this study achieves an appropriate rate of decrease in size by using this form of fractal geometry. The suggested filter has a frequency range between 7.7 and 9.65 GHz.

The proposed filter was simulated using three industry-standard numerical electromagnetic calculation software programs to validate the findings. The suggested filter structure is implemented with promising results.

References

[1] D. Deslandes, "Substrate Integrated Waveguide Leaky-Wave Antenna: Concept and Design Considerations," *Asia Pacific Microwave Conference Proceedings*, vol. 1, pp. 346-349, 2005. [Google Scholar] [Publisher Link]

[2] M. Bozzi, A. Georgiadis, and K. Wu, "Review of Substrate-Integrated Waveguide Circuits and Antennas," *IET Microwaves, Antennas & Propagation*, vol. 5, no. 8, pp. 909-920, 2011. [CrossRef] [Google Scholar] [Publisher Link]

[3] N. Grigoropoulos, B. Sanz-Izquierdo, and P.R. Young, "Substrate Integrated Folded Waveguides (SIFW) and Filters," *IEEE Microwave and Wireless Components Letters*, vol. 15, no. 12, pp. 829-831, 2005. [CrossRef] [Google Scholar] [Publisher Link]

[4] Xiao-Ping Chen, Ke Wu, and Zhao-Long Li, "Dual-Band and Triple-Band Substrate Integrated Waveguide Filters with Chebyshev and Quasi-Elliptic Responses," *IEEE Transactions on Microwave Theory and Techniques*, vol. 55, no. 12, pp. 2569-2578, 2007. [CrossRef] [Google Scholar] [Publisher Link]

[5] Xiao-Ping Chen, and Ke Wu, "Substrate Integrated Waveguide Cross-Coupled Filter with Negative Coupling Structure," *IEEE Transactions on Microwave Theory and Techniques*, vol. 56, no. 1, pp. 142-149, 2008. [CrossRef] [Google Scholar] [Publisher Link]

[6] Maurizio Bozzi et al., "Current and Future Research Trends in Substrate Integrated Waveguide Technology," *Radioengineering*, vol. 18, no. 2, pp. 201-209, 2009. [Google Scholar] [Publisher Link]

[7] W. Che et al., "Investigations on Propagation and the Band Broadening Effect of Ridged Rectangular Waveguide Integrated in a Multilayer Dielectric Substrate," *IET Microwaves, Antennas & Propagation*, vol. 4, no. 6, pp. 674-684, 2010. [CrossRef] [Google Scholar] [Publisher Link]

[8] Qinghua Lai et al., "Characterization of the Propagation Properties of the Half-Mode Substrate Integrated Waveguide," *IEEE Transactions on Microwave Theory and Techniques*, vol. 57, no. 8, pp. 1996-2004, 2009. [CrossRef] [Google Scholar] [Publisher Link]

[9] Dong-Won Kim, and Jeong-Hae Lee, "A Partial H-Plane Waveguide as a New Type of Compact Waveguide," *Microwave and Optical Technology Letters*, vol. 43, no. 5, pp. 426-428, 2004. [CrossRef] [Google Scholar] [Publisher Link]

[10] Amjad Iqbal et al., "Miniaturization Trends in Substrate Integrated Waveguide (SIW) Filters: A Review," *IEEE Access*, vol. 8, pp. 223287-223305, 2020. [CrossRef] [Google Scholar] [Publisher Link]

[11] J.P. Gianvittorio, and Y. Rahmat-Samii, "Fractal Antennas: A Novel Antenna Miniaturization Technique, and Applications," *IEEE Antennas and Propagation Magazine*, vol. 44, no. 1, pp. 20-36, 2002. [CrossRef] [Google Scholar] [Publisher Link]

[12] Basudeb Ghosh et al., "Bandpass Characteristics of Substrate Integrated Waveguide Loaded with Hilbert Curve Fractal Slot," *IEEE iWEM2011*, Taipei, Taiwan, pp. 89-93, 2011. [CrossRef] [Google Scholar] [Publisher Link]

[13] Vikram Sekar, and Kamran Entesari, "Miniaturized Half-Mode Substrate Integrated Waveguide Bandpass Filters Using Cross-Shaped Fractals," *WAMICON 2011 Conference Proceedings*, Clearwater Beach, FL, USA, pp. 1-5, 2011. [CrossRef] [Google Scholar] [Publisher Link]

[14] Sheng Zhang et al., "Novel Fractal-Shaped Bandpass Filter Using Quarter Substrate Integrated Waveguide Resonator (QSIWR)," *2011 4th IEEE International Symposium on Microwave, Antenna, Propagation and EMC Technologies for Wireless Communications*, Beijing, China, pp. 171-174, 2011. [CrossRef] [Google Scholar] [Publisher Link]

[15] Sheng Zhang et al., "Quarter Substrate Integrated Waveguide Resonator Applied to Fractal-Shaped BPFs," *Microwave Journal*, 2012. [Google Scholar] [Publisher Link]

[16] Michele A. Chiapperino et al., "Dual-Band Substrate Integrated Waveguide Resonator Based on Sierpinski Carpet," *Progress in Electromagnetics Research C*, vol. 57, pp. 1-12, 2015. [CrossRef] [Google Scholar] [Publisher Link]

[17] Juan de Dios Ruiz et al., "Substrate Integrated Waveguide (SIW) with Koch Fractal Electromagnetic Bandgap Structures (KFEBG) for Bandpass Filter Design," *IEEE Microwave and Wireless Components Letters*, vol. 25, no. 3, pp. 160-162, 2015. [CrossRef] [Google Scholar] [Publisher Link]

[18] Jun-Ping Liu, Zhi-Qing Lv, and Xiang An, "Compact Substrate Integrated Waveguide Filter Using Dual-Plane Resonant Cells," *Microwave and Optical Technology Letters*, vol. 58, no. 1, pp. 111-114, 2016. [CrossRef] [Google Scholar] [Publisher Link]

[19] Sheng Zhang et al., "Quasi Quarter SIW-Mode Resonator and Its Application to Sierpinski Fractal Filter Design," *Microwave and Optical Technology Letters*, vol. 58, no. 5, pp. 1176-1179, 2016. [CrossRef] [Google Scholar] [Publisher Link]

[20] Sheng Zhang et al., "Quasi Eighth-Mode Substrate Integrated Waveguide (SIW) Fractal Resonator Filter Utilizing Gap Coupling Compensation," *Frequenz*, vol. 70, no. 9-10, pp. 377-380, 2016. [CrossRef] [Google Scholar] [Publisher Link]

[21] Mostafa Danaeian, and Hossein Ghayoumi-Zadeh, "Miniaturized Substrate Integrated Waveguide Filter Using Fractal Open Complementary Split-Ring Resonators," *International Journal of RF and Microwave Computer-Aided Engineering*, vol. 28, no. 5, 2018. [CrossRef] [Google Scholar] [Publisher Link]

[22] Nitin Muchhal, and Shweta Srivastava, "Design of Miniaturized High Selectivity Folded Substrate Integrated Waveguide Band Pass Filter with Koch Fractal," *Electromagnetics*, vol. 39, no. 8, pp. 571-581, 2019. [CrossRef] [Google Scholar] [Publisher Link]

[23] Ayad Muslim Hamzah, Lukman Audah, and Nasr Alkhafaji, "H-Shaped Fractal Slots Based Highly Miniaturized Substrate Integrated Waveguide Metamaterial Bandpass Filters for C-Band Applications," *Progress in Electromagnetics Research B*, vol. 86, pp. 139-158, 2020. [CrossRef] [Google Scholar] [Publisher Link]

[24] Nitin Muchhal et al., "Miniaturized and Selective Half-Mode Substrate Integrated Waveguide Bandpass Filter Using Hilbert Fractal for Sub-6 GHz 5G Applications," *IETE Journal of Research*, pp. 1-8, 2022. [CrossRef] [Google Scholar] [Publisher Link]

[25] Mohammed El Amine Chaib et al., "Bandpass Filters Based on Hybrid Structure of Substrate Integrated Waveguide (SIW) and Hilbert Defected Ground Structure (HDGS)," *Progress in Electromagnetics Research Letters*, vol. 104, pp. 27-35, 2022. [CrossRef] [Google Scholar] [Publisher Link]

[26] Nitin Muchhal et al., "Design of Hybrid Fractal Integrated Half Mode SIW Bandpass Filter with CSRR and Minkowski Defected Ground Structure for Sub-6 GHz 5G Applications," *Photonics*, vol. 9, no. 12, pp. 1-11, 2022. [CrossRef] [Google Scholar] [Publisher Link]

[27] Mohammed El Amine Chaib et al., "Miniaturized and Optimized Half Mode SIW Bandpass Filter Design Integrating Hilbert Cells as DGS," *Electromagnetics*, vol. 43, no. 3, pp. 211-219, 2023. [CrossRef] [Google Scholar] [Publisher Link]

[28] M. Sanchez-Renedo, and R. Gomez-Garcia, "Multi-Coupled-Resonator Dual-Band Bandpass Microstrip Filters with Non-Resonating Nodes," *2011 IEEE MTT-S International Microwave Symposium*, Baltimore, MD, USA, pp. 1-1, 2011. [CrossRef] [Google Scholar] [Publisher Link]

[29] Ping-Juan Zhang, and Min-Quan Li, "Cascaded Trisection Substrate-Integrated Waveguide Filter with High Selectivity," *Electronics Letters*, vol. 50, no. 23, pp. 1717-1719, 2014. [CrossRef] [Google Scholar] [Publisher Link]

[30] Amit Ranjan Azad, Dharmendra Kumar Jhariya, and Akhilesh Mohan, "Substrate-Integrated Waveguide Cross-Coupled Filters with Mixed Electric and Magnetic Coupling Structure," *International Journal of Microwave and Wireless Technologies*, vol. 10, no. 8, pp. 896-903, 2018. [CrossRef] [Google Scholar] [Publisher Link]

[31] L. Wu et al., "Design of Substrate Integrated Waveguide (SIW) Elliptic Filter with Novel Coupling Scheme," *Journal of Electromagnetic Waves and Applications*, vol. 26, no. 5-6, pp. 827-835, 2012. [CrossRef] [Google Scholar] [Publisher Link]

[32] Pratik Mondal, and Susanta Kumar Parui, "Design of Higher Order Miniaturized Bandpass Filter Using Two Cascaded New Multimode Resonators," *2017 IEEE Asia Pacific Microwave Conference (APMC)*, Kuala Lumpur, Malaysia, pp. 813-816, 2017. [CrossRef] [Google Scholar] [Publisher Link]

[33] Jia-Sheng Hong, and M.J. Lancaster, *Microstrip Filters for RF/Microwave Applications*, John Wiley & Sons, 2004. [CrossRef] [Google Scholar] [Publisher Link]